Performances Comparison of 12S-14P Field Excitation Flux Switching Motor with Overlap and Non-overlap Windings for Hybrid Electric Vehicles

Zhafir Aizat Husin, Erwan Sulaiman, Faisal Khan and Mohd Fairoz Omar
Department of Electrical Power Engineering
Universiti Tun Hussein Onn Malaysia, Locked Bag 101
Batu Pahat, Johor, 86400 Malaysia
zhafiraizat69@gmail.com and erwan@uthm.edu.my

***Abstract*—Hybrid electric vehicles (HEVs), using combination of an internal combustion engine (ICE) and one or more electric motors, are widely considered as the most promising clean vehicles. The only machine that already installed for HEVs is interior permanent magnet synchronous machine (IPMSM) where it has developed to enhance power density of the machine. Despite of fine operated and superior performances, this machine do not miss approached by deficiency for instance IPMSM now have complex form and configuration that give difficulty to undertake the process of optimization. Moreover, the use of PM will result in a constant state of flux and cannot be controlled as well a burden because of expensive rare earth magnet prices. Therefore, a new candidate of field excitation flux switching machine (FEFSM), in which the uses of PM are totally excluded with rugged rotor structure suitable for high-speed operation and the ability to keep high torque and power density is proposed and examined in this paper. Under some design specifications, design principles and performances of 12S-14P FEFSMs with overlap and non-overlap FEC and armature coil windings are presented. The profile of flux linkage, induced voltage, cogging torque, torque and power characteristics are observed based on 2D finite element analysis (FEA).**

Keywords—Field Excitation Flux Switching Motor, Hybrid Electric Vehicle and Field Excitation Coil (DC FEC)

I. INTRODUCTION

In the mid 1950s, the initial concept of flux switching motor (FSM) has been published. In general, permanent magnet flux switching motor (PMFSM), field excitation flux switching motor (FEFSM), and hybrid excitation flux switching motor (HEFSM) are three types of FSM as illustrate in Fig. 1. Both FEFSM and PMFSM has only permanent magnet and field excitation coil (FEC), correspondingly as the main source of flux, whilst HEFSM combines both FEC and permanent magnet as their main flux sources.

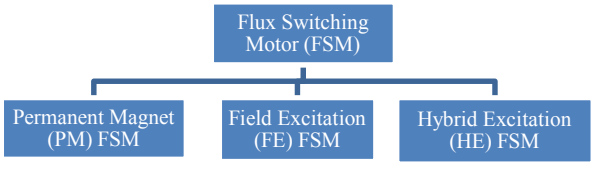

Fig. 1. Classifications of flux switching machine

Permanent magnet (PM) machines exhibit high torque density and high efficiency but the rare earth magnet material is expensive and the working environmental temperature may limit its application. In fact, the flux-weakening operation at high speed is relatively difficult for PM machines due to fixed PM excitation. In order to reduce the cost, one of the possible solutions is to replace the magnet excitation by the field excitation (FE). The conventional FE synchronous machine employs the FE on the rotor, and, consequently, the slip-rings are required to supply the field current. The FE doubly salient machine has been proposed the hybrid excited doubly salient and PMFSM have been investigated [1]-[3]. In addition, an FE flux switching machine (FEFSM) with modular rotor and non-overlapping windings has been recently investigated [4]. Although it has been mentioned that the magnets could be replaced by the FE in three-phase PMFSM, the three-phase FEFSM has not further investigated.

Moreover, the use of PM will result in a constant state of flux and cannot be controlled as well a burden because of expensive rare earth magnet prices. The one-phase FEFSM has been proposed and analyzed for automotive application due to extremely low cost of the machine [5]. The design principle and the one-phase FEFSM has been shown to exhibit a higher output power density than the equivalent universal and induction machines, and comparable efficiency to that of the induction machine [6]. However, the one-phase FEFSM has problems of low starting torque, large torque ripple, and fixed rotating direction. Thus, three-phase FEFSM with a new form has been created as a new candidate that can address these problems in which the uses of permanent magnet is totally excluded while the field excitation coil (FEC) is located on the stator [7]-[9]. The proposed motor has a simple and easy structure and it is expected to provide much higher power density and torque [10]-[12].

The motor is operated based on the principle of switching flux and to describe machines in which the stator tooth flux switches polarity following the motion of a salient pole rotor [13]. The principle operation of FEFSM is demonstrated in Fig. 2. Fig. 2 (a) and (b) show the movement of the FEC flux into the rotor while (c) and (d) visualize the movement of FEC flux into the stator which creates one complete cycle movement of fluxes. The stator fluxes switches between the alternate stator

978-1-4799-6428-4/14/$31.00 ©2014 IEEE

teeth because of the each reversal of armature current shown by the transition involving Fig. 2 (a) and (b) [14].

II. Review on Electric Motors used in HEV

Hybrid Electric Vehicles (HEVs), by means of merge of an Internal Combustion Engine (ICE) plus another electric traction motors are mostly consider as the primarily proficient green vehicles.

There are four major types of electric machines currently used in HEV drives namely DC machine, induction machine (IMs), switch reluctance machine (SRMs) and also permanent magnet synchronous machines (PMSMs) as depicted in Fig. 3. However, there exist several drawbacks in each motor.

Firstly, DC motor is unfavorable because this kind of motor comes out with huge structure, low reliability and low efficiency [15]-[16]. Next, IM drives encompass drawbacks for example low efficiency, high loss, low inverter-usage factor and low power factor which are more concern for the large power and high power motor and that pressed them away from the battle of HEVs electric propulsion system [17] and SRMs are familiarly known to have high torque ripple and acoustic noise generation [18]-[19]. In addition, PMSMs have a low impact on the efficiency at the high-speed range due to the enhance amount in iron loss as well as risk of magnetic faults [20].

The only machine that already installed for HEVs is interior PMSMs (IPMSMs) where it has developed to enhance power density of the machine [21]-[22] but it have complex form and configuration that give difficulty to undertake the process of optimizing the design of this motor. Moreover, the use of PM will result in a constant state of flux and cannot be controlled as well a burden because of expensive rare earth magnet prices.

III. Design Restrictions, Specifications and Parameters of FEFSM

The motor parameters, restrictions and target specifications of the projected FEFSM for HEV applications are scheduled in Table I. The inverter is set at the maximum of 650V DC bus voltage as well as inverter current at 360V. Assuming water jacket system is in use as the cooling system for the machine the limit of the current density is set to the maximum 30Arms/mm^2 for armature winding and 30A/mm^2 for FEC, respectively. The motor stack length, the outer diameter, the air gap and the shaft radius of the major parts of the machine design being 70mm, 264mm, 0.8mm and 30mm, respectively, alike with existing IPMSMs. The electrical steel 35H210 is used for stator and rotor body.

The numbers of turns of FEC and armature coil are defined from (1) and (2), respectively. The motor's filling factor is put at 0.5, whilst the slot area of armature slot and FEC slot is calculated, correspondingly. To ensure flux moves from stator to rotor equally without any flux leakage, the design of the proposed machine is defined as in (3). The rotor is consisted of only stacked soft iron sheets and can be expected to rotate at high-speed because the rotor structure is mechanically robust. The motor weight to be intended is below 35kg, ensuring in that the projected FEFSM assures to attain the maximum power density more than 3.5kW/kg, better in contrast with

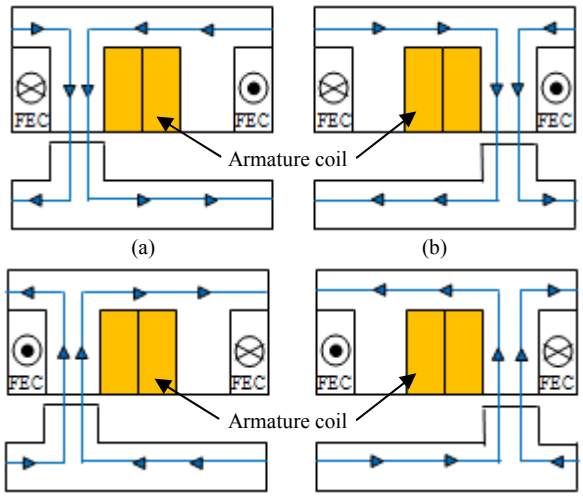

Fig. 2. Operating principle of FEFSM (a) θe=0° and (b) θe=180° fluxes move from stator to rotor (c) θe=0° and (d) θe=180° fluxes move from rotor to stator

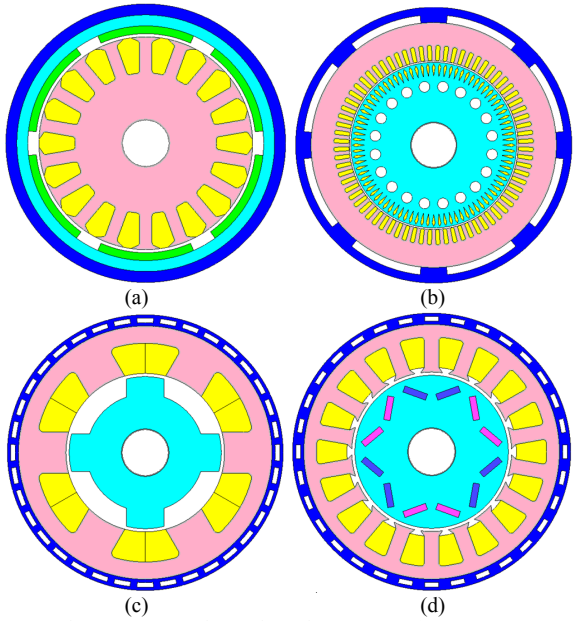

Fig. 3. Cross sections of traction motors (a) DC motor (b) induction motor (c) switch reluctance motor (d) interior PMSM

TABLE I. FEFSM Propose Specifications and Limitations

Items	IPMSMs	FEFSMs
Max. inverter DC-bus voltage (V)	650	650
Max. current of inverter (A_{rms})	Confidential	360
Armature winding J_a, maximum current density (A_{rms}/mm^2)	Confidential	30
Excitation winding J_e, maximum current density (A/mm^2)	NA	30
Stack length of motor (mm)	70	70
Outer diameter of stator (mm)	264	264
Length of air gap (mm)	0.8	0.8
Radius of shaft (mm)	30	30
Weight of PM (kg)	1.1 (est.)	0
Maximum torque (Nm)	333	> 210
Maximum power (kW)	123	> 123
Power density (kW/kg)	3.5	> 3.5

existing IPMSMs. Furthermore, the maximum expected torque of 210Nm and power is set to be higher than 123kW, respectively. The commercial finite element analysis (FEA) package, JMAG-Designer ver.13.0, released by Japan Research Institute is used as 2D-FEA solver in this design.

$$N_a = \frac{J_a \alpha S_a}{I_a} \tag{1}$$

$$N_e = \frac{J_e \alpha S_e}{I_e} \tag{2}$$

$$S_W = R_W \tag{3}$$

Where *N, J, α, S* and *I* are number of turns, current density, filling factor, slot area and input current, respectively. For the subscript *a* and *e* represent armature coil and FEC, respectively. The machine configurations of 12 stator slots and 14 pole numbers with overlap plus non-overlap windings is illustrated as in Fig. 4. The FEC directions are in alternate direction, counter-clockwise polarity and clockwise polarity, respectively.

Primarily, the selection of the proposed FEFSM is designed with the following assumptions; (i) The inner radius is set to 30 mm for the motor's shaft while rotor radius is 97.2 mm which is 73% of 132 mm motor radius and within the range of general machine split ratio, (ii) The stator outer core thickness is set to be half of the stator inner length with the assumptions that the fluxes are divided into two parts, (iii) The depth of the rotor pole is set to be 1/3 of rotor radius to give much depth for the flux to flow, (iv) The FEC and armature coil slot opening angle are set to 3.75°, which is half of the stator slot opening angle of 7.5°, (v) The total coil slot area of both FEC and armature coil is less than the stator teeth area. Therefore, it is expected that all fluxes from both coils to have sufficient space to flow in the stator yoke, without magnetic saturation.

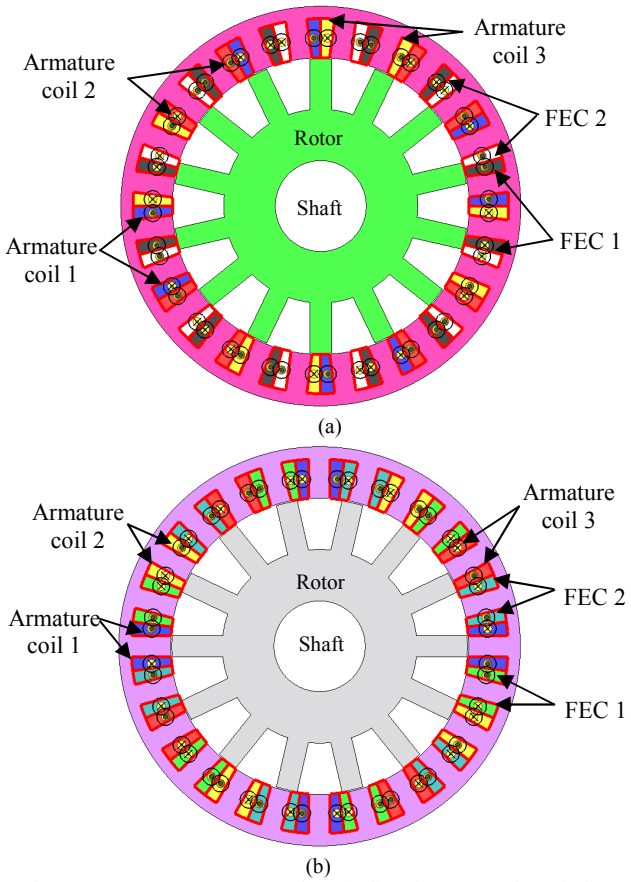

Fig. 4. 12S-14P FEFSM (a) overlap winding (b) non-overlap winding

IV. Design Performance and Results Based on 2D Finite Element Analysis

A. Coil Arrangement Test

Coil arrangements are examined in each armature coil slots singly in order to verify the principle operation of the FEFSM and to set the arrangement of each armature coil phase, where all armature coils are wounded in counter-clockwise direction while FEC are wounded in alternate direction, counter-clockwise polarity and clockwise polarity, respectively. The flux linkages of overlap and non-overlap windings FEFSM at each coil are observed and the armature coil phases are defined according to the conservative three-phase as U, V, and W, respectively as demonstrated in Fig. 5.

As seen from the graph, FEFSM with overlap winding produce higher flux than non- overlap winding as the flux produce is relatively smooth as no distortion. Thus, it is expected that FEFSM with overlap winding will produce much higher torque and power. The armature coil flux can start the rotor at the maximum as the U flux satisfies the zero rotor position indicated by red dotted line.

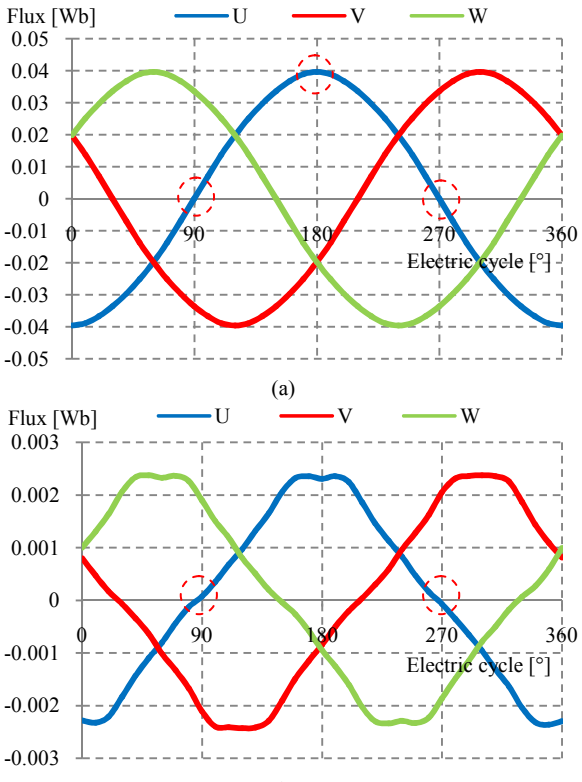

Fig. 5. 3-phase flux of 12S-14P FEFSM (a) overlap winding (b) non-overlap winding

B. *FEC Flux Linkage at various FEC current density, J_E*

The DC FEC flux linkage at various DC FEC current densities, J_E are also investigated as illustrated in Fig. 6 to 7, respectively. From the figures, it is clear that initially the flux pattern is increased with the increase in DC FEC current density, J_E. However, the flux generated starts to reduce when higher DC FEC current density is injected to the system as demonstrated in Fig. 7. It is expected that this phenomena occurs due to some flux leakage and flux cancellation that will be investigated in future. In addition, the flux generated from overlap winding is higher than non-overlap FEFSM.

The flux distribution at zero rotor position of DC FEC for both overlap and non-overlap FEFSM are illustrated in Fig. 8. From the figure, it is depicted that the large amount of flux easily flow from stator to rotor and back to stator in overlap winding while for non-overlap winding at the same amount of current, the flux linkage is less and the stator core gets saturated as indicated by red circle. The flux linkage of 12S-14P with non-overlap winding can be improved by design refinement and optimization.

C. *Induced Voltage at Open Circuit Condition*

The fundamental of induced voltage generated for overlap and non-overlap winding of 12S-14P are presented in Fig. 12. The induced voltage generated from DC FEC flux is at open circuit condition of both FEFSM at maximum DC FEC current densities, J_E. As illustrates from the graph, overlap 12S-14P has higher value of induced voltage compared to non-overlap 12S-14P FEFSMs.

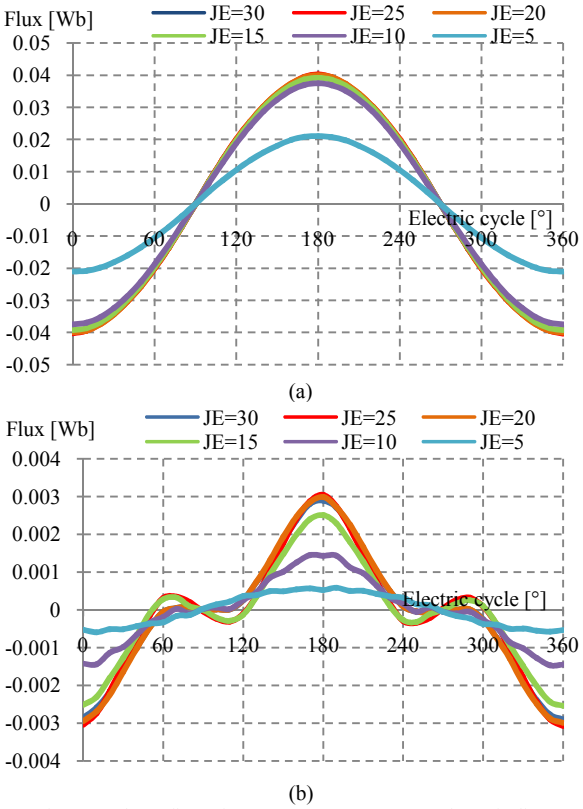

Fig. 6. 3-phase flux of 12S-14P FEFSM (a) overlap winding (b) non-overlap winding

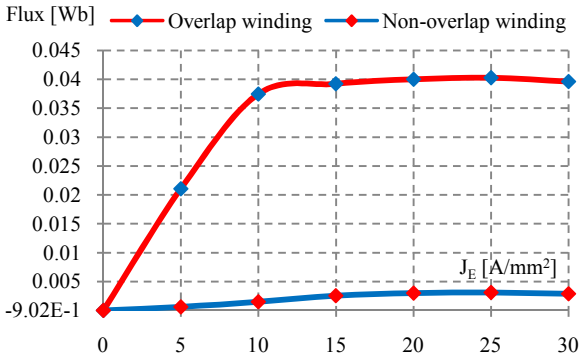

Fig. 7. Maximum U flux at various J_E

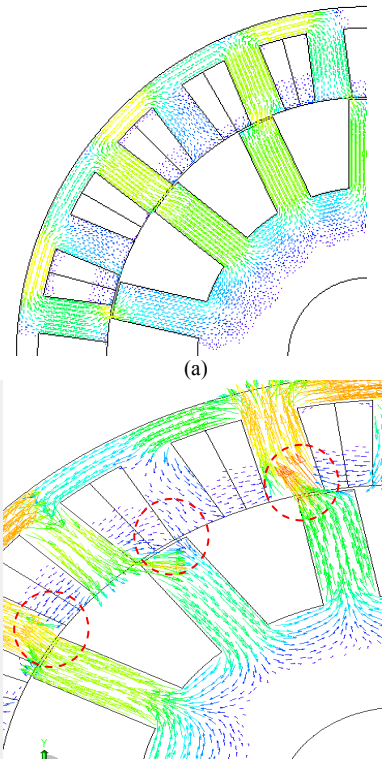

Fig. 8. Flux distribution of FEFSM (a) overlap winding (b) non-overlap winding

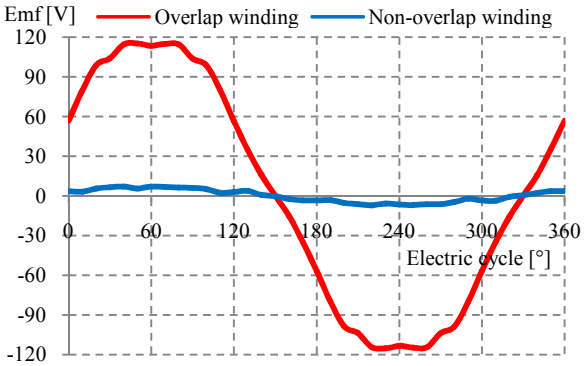

Fig. 9. Induced voltage of 12S-14P FEFSM

The value of induced voltage must not exceed the supply voltage, 650V because it will interrupt the operation of the motors as it is use for regenerative breaking to charge battery. Basically, motor will not definitely stop when it trip because of the DC supply but there will be changes of flux. Hence, this phenomena will create induce voltage based on Faraday's Law.

D. Cogging Torque

The torque ripple feature for FEFSMs is shown in Fig. 10. From the graph, is evidence that 12S-14P with non-overlap winding has highest peak to peak torque ripple in contrast with overlap winding 12S-14P FEFSM with 18.5Nm and 5.2Nm, correspondingly. High vibration and noise will occur and effect FEFSM's performances as if the cogging torque exceeds 10% of the average torque produced.

E. Instantaneous Torque and Power Characteristics

At last, by situate the armature coil current density, J_A at maximum conditions, the torque profile and power at a variety of FEC current densities, J_E is depicted in Fig. 11 to 13. From the figure, it is revealed that the highest torque and power appear at 12S-14P overlap winding about 226.1Nm and 127.6kW, respectively followed by non-overlap 12S-14P FEFSM with torque of 43.04Nm and power of 5.41kW. The reason behind this is because negative torque is produced due to cancellation of fluxes between FECs and armature coils. It is necessary to do further investigation to identify the problem on these non-overlap winding configurations. Additionally for non-overlap winding, the torque and power is still distant from the target requirements. In order to suit the goal, design refinement and optimization based on deterministic approach will be conducted in the future until the intention power and torque are attained [23]-[25].

V. CONCLUSION

Design study and analysis comparison of 12 stator slots and 14 pole numbers with overlap plus non-overlap windings FEFSMs for traction drive in HEV applications has been proposed and concluded as in Table II. The proposed machine has no PM and in consequence, it can be anticipated as very cost-effective machine as well as simple structure. In addition, the generated flux can be controlled with variable capabilities through the presence of FEC. Thus, by advance design refinement, modification and optimizations, the target performance of FEFSMs are anticipated can be attained.

TABLE II. OVERALL PERFORMANCE OF 12S-14P FEFSMS

	Target	Overlap	Non-overlap
T (Nm)	>210	226.1	43.04
P (Kw)	>123	127.6	5.41
Weight (kg)	<35	25	25
Pd (Kw/kg)	>3.51	5.1	0.2
Td (Nm/Kg)	>6	9.04	1.72

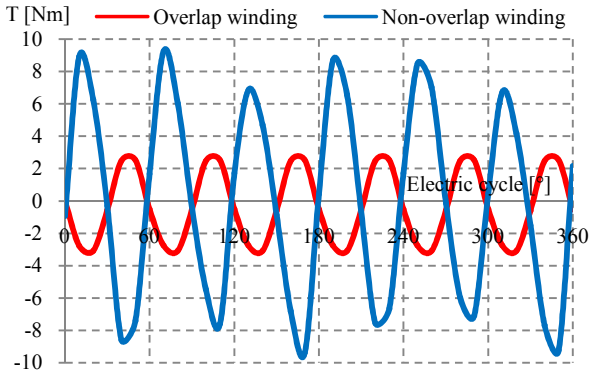

Fig. 10. Cogging torque

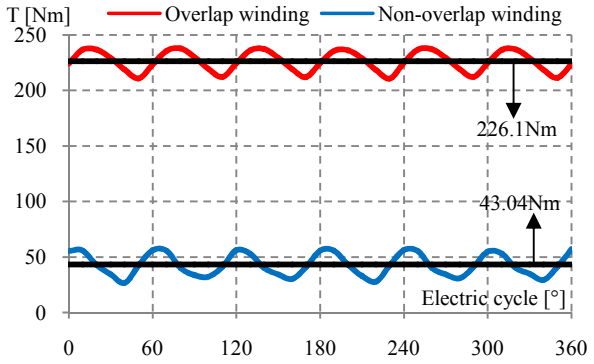

Fig. 11. Instantaneous torque characteristics of FEFSMs

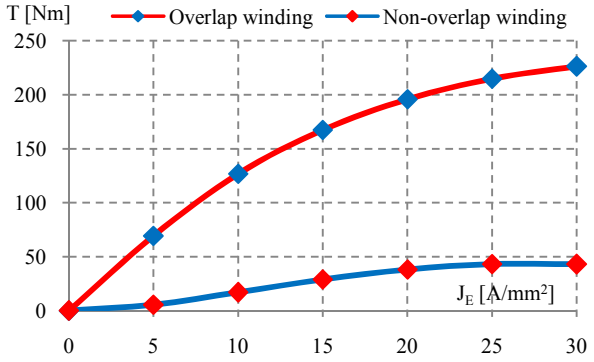

Fig. 12. Torque vs J_E at maximum J_A

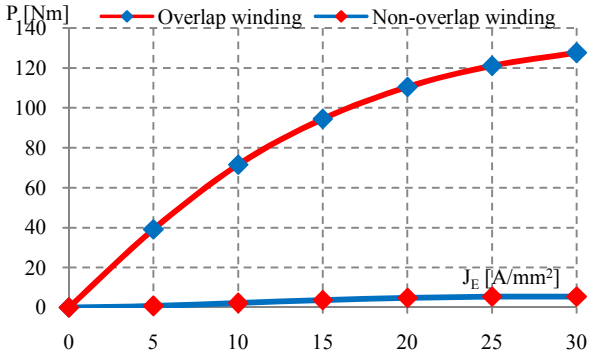

Fig. 13. Power vs J_E at maximum J_A

ACKNOWLEDGMENT

This research was supported by ERGS (Vot E030) under Research, Innovation, Commercialization and Consultancy Management (ORICC) UTHM, Batu Pahat and Ministry of Higher Education Malaysia (MOHE).

REFERENCES

[1] Y. Fan, K. T. Chau, and S. Niu, "Development of a New Brushless Doubly Fed Doubly Salient Machine For Wind Power Generation," IEEE Trans. Magnetics, vol. 42, no. 10, pp. 3455-3457, Oct. 2006.

[2] Y. Li and T. A. Lipo, "A Doubly Salient Permanent Magnet Motor Capable of Field Weakening," Proc. IEEE Power Electronics Specialists Conf., vol. 1, June 1995, pp. 565-571.

[3] E. Hoang, M. Lecrivain, and M. Gabsi, "A New Structure of a Switching Flux Synchronous Polyphased Machine with Hybrid Excitation," Proc. Eur. Conf. Power Electronics and Applications, pp1–8, Sept. 2007.

[4] Shinji Nishimura, "Dynamo-Electric Machine," United States Patent, US 6,495,941, Dec. 2002.

[5] C. Pollock, H. Pollock, R. Barron, J. R. Coles, D. Moule, A. Court, and R. Sutton, "Flux-Switching Motors For Automotive Applications," IEEE Tran. Ind. Appl., vol. 42, no. 5, pp. 1177-1184, Sept. /Oct. 2006.

[6] J. F. Bangura, "Design of High-Power Density and Relatively High Efficiency Flux-Switching Motor," IEEE Trans. Ener. Conv., vol. 21, no.2, pp. 416-425, June 2006.

[7] E. Sulaiman, T. Kosaka, and N. Matsui, "A New Structure of 12Slot-10Pole Field-Excitation Flux Switching Synchronous Machine for Hybrid Electric Vehicles", Proc. of 14th European Conference on Power Electronics and Applications, Birmingham, Sept. 2011.

[8] E. Sulaiman, T. Kosaka, and N. Matsui, "Design Study and Experimental Analysis of Wound Field Flux Switching Motor for HEV Applications", XXth IEEE Int. Conf. on Electrical Machines (ICEM 2012), Marseille, France, Sept 2012.

[9] E. Sulaiman, M. F. M. Teridi, Z. A. Husin, M. Z. Ahmad and T. Kosaka, "Performances Comparison of 24s-10p and 24s-14p Field Excitation Flux Switching Machine (FEFSM) With Single DC-Coil Polarity", International Journal of Energy & Power Engineering Research, Vol, 1, pp. 24-31, Dec 2013.

[10] E. Sulaiman, T. Kosaka, and N. Matsui, "Design and Analysis of High-Power/ High-Torque Density Dual Excitation Switched-Flux Machine for Traction Drive in HEVs", Renewable & Sustainable Energy Review, submitted for 3rd review, Jan 2014.

[11] E. Sulaiman, T. Kosaka, N. Matsui, and M. Z. Ahmad, "Design Studies on High Torque and High Power Density Hybrid Excitation Flux Switching Synchronous Motor for HEV Applications," in IEEE International Power Engineering and Optimization Conference (PEOCO), 2012, pp. 333–338, June 2012.

[12] E. Sulaiman, T. Kosaka, and N. Matsui: "High power density design of 6slot-8pole hybrid excitation flux switching machine for hybrid electric vehicles", IEEE Trans. on Magn., vol.47, no.10 pp. 4453-4456, Oct. 2011.

[13] S. E. Rauch and L.J. Johnson, 'Design principles of flux-switch alternators', Tans. AIEE, vol. 74 pt. III, pp. 1261-1268, 1955.

[14] E. Sulaiman, "Less Rare-Earth and High Power Density Flux Switching Motor for HEV Drives, International Conference on Electrical machine ICEM pp. 15-23, June 2012.

[15] A. Emadi, J. L.Young, K.Rajashekara, "Power electronics and motor drives in electric, hybrid electric, and plug-in hybrid electric vehicles", IEEE Trans. Ind. Electron., vol.55, no.6, pp.2237-2245, Jan. 2008.

[16] D. W. Gao, C. Mi, and A. Emadi, "Modeling and simulation of electric and hybrid vehicles", Proc. IEEE, vol. 95, no. 4, pp. 729–745, April 2007.

[17] T. Wang et al., "Design characteristics of the induction motor used for hybrid electric vehicle," IEEE Trans. Magn., vol. 41, no. 1, pp. 505–508, Jan. 2005.

[18] J. Malan and M. J. Kamper, "Performance of a hybrid electric vehicle using reluctance synchronous machine technology", IEEE Trans. Ind.Appl., vol. 37, no. 5, pp. 1319–1324, Sep./Oct. 2001.

[19] K. M. Rahman, B. Fahimi, G. Suresh, A. V. Rajarathnam, and M. Ehsani, "Advantages of switched reluctance motor applications to EV and HEV: Design and control issues", IEEE Trans. Ind. Appl., vol. 36, no. 1, pp. 111–121, Jan./Feb. 2000.

[20] T. M. Jahns, and V. Blasko, "Recent advances in power electronics technology for industrial and traction machine drives", Proc. IEEE, vol. 89, no. 6, pp. 963–975, June 2001.

[21] M. Kamiya: "Development of traction drive motors for the Toyota hybrid systems", IEEJ Transaction on Industry Applications, vol.126, no.4, pp.473-479, April 2006.

[22] M.A. Rahman: "IPM Motor Drives For Hybrid Electric Vehicles", InternationalAegean Conference on Electrical Machines and Power Electronics, Sept. 2007.

[23] X. D. Xue, K. W. E. Cheng, T. W. Ng, N. C. Cheung, "Multi objective optimization design of in-wheel switched reluctance motors in electric vehicles", IEEE Trans. Ind. Electron., vol.57, no.9, pp.2980-2987, Sept. 2010.

[24] E. Sulaiman, T. Kosaka, and N. Matsui, "Design optimization and performance of a novel 6-Slot 5-Pole PMFSM with hybrid excitation for Hybrid Electric Vehicle", IEEJ Trans. on Industry Appl., vol. 132, No. 2, Sec. D, pp. 211-218, 2012.

[25] E. Sulaiman, T. Kosaka, and N. Matsui, "FEA-based Design and Parameter Optimization Study of 6-slot 5-pole PMFSM with Field Excitation for Hybrid Electric Vehicle," IEEE International Conference on Power and Energy (PECon 2010) pp. 206-201, Dec 2010.